

# Design of multifunctionalized mesoporous silicas for esterification of fatty acid

Isa K. Mbaraka, Brent H. Shanks \*

*Department of Chemical Engineering, Iowa State University, Ames, IA 50011, USA*

Received 26 July 2004; revised 4 November 2004; accepted 8 November 2004

Available online 23 December 2004

## Abstract

Organosulfonic acid mesoporous silicas further functionalized with hydrophobic organic groups were synthesized via postsynthesis grafting and one-step co-condensation methods. The resulting materials were tested in the esterification of fatty acid with methanol to produce methyl esters as a pretreatment step in the production of biodiesel. Incorporation of the hydrophobic group into the organic–inorganic hybrid acid catalyst was found to improve the performance of the resulting catalyst. However, the performance of the multifunctionalized mesoporous materials demonstrated a strong dependence on the incorporation method and on the size of the hydrophobic organic groups. Solution effects within the reaction mixture appeared to influence the catalytic activity of the catalysts. The results indicate the potential for intentional design of the catalytic environment at a molecular level with the use of organic–inorganic mesoporous materials.

© 2004 Elsevier Inc. All rights reserved.

**Keywords:** Multifunctionalized mesoporous silicas; Organic–inorganic hybrid catalysts; Fatty acid esterification; Methyl esters

## 1. Introduction

Organic–inorganic hybrid silicas synthesized by supramolecular assembly have received increasing attention because of their high surface area, flexible pore sizes, and their potential for controlling catalytic functionalities at the molecular level [1–4]. These mesostructured materials can be tailored for application by the incorporation of specific organofunctionalized groups onto the surface of the inorganic framework, which would modify the physical and chemical properties of the metal oxide supports at the nanoscale to the desired application requirements, such as separation, chemical sensing, adsorption, and catalysts. In solid acid catalysis, zeolites are widely used, but they are limited to pores in the microporous range ( $< 15 \text{ \AA}$ ) that are not accessible by large reactants. Incorporation of organosulfonic acid groups into mesoporous materials to create a solid acid catalyst has been explored as a means of increasing

the pore size range available for heterogeneous acidic catalysts [5–7]. In addition to the flexibility in pore diameter, the performance of organosulfonic acid-functionalized mesoporous silica can be improved by the selective exclusion of unwanted molecules that can inhibit the reactants from approaching active sites [8–10]. This attribute is particularly important to the processing of biobased reactants, which commonly have impurities that require pretreatment prior to catalytic chemical conversion [11].

One such application is the esterification of free fatty acids with acidic catalysts as a pretreatment step in the production of biodiesel [12–14]. Biodiesel has been the subject of extensive interest as a result of its desirable renewable, biodegradable, and nontoxic properties [15–17]. Generally, biodiesel is produced via the transesterification of vegetable oils with short-chain alcohols (e.g., methanol) to form alkyl esters that have properties similar to those of fossil-derived diesel [18,19]. However, biodiesel is currently not cost competitive with conventional diesel fuel because of its high raw material and production costs. To improve biodiesel economics, feedstock selection becomes critical. The con-

\* Corresponding author. Fax: 515-294-2689.  
E-mail address: [bshanks@iastate.edu](mailto:bshanks@iastate.edu) (B.H. Shanks).

ventional biodiesel feeds, vegetable oils, are more expensive than oil feeds containing high free fatty acid content, as found in beef tallow or yellow grease. Unfortunately, utilization of these high-free-fatty-acid feeds in traditional biodiesel production processes leads to depletion of the catalysts as well as increased purification costs, since the free fatty acid is saponified by the homogeneous alkaline catalyst, producing excess soap [20].

The free fatty acid processing problem can be circumvented by an esterification pretreatment of the free fatty acids to alkyl esters in the presence of an acidic catalyst. The pretreated oils in which the free fatty acid content is lowered to no more than 0.5 wt% can then be processed under standard transesterification reaction conditions [12]. Koono et al. [21] successfully demonstrated the pretreatment step with the use of sulfuric acid; however, the use of a homogeneous acidic catalyst adds neutralization and separation steps to the process. It would be advantageous to use a heterogeneous acidic catalyst in the esterification pretreatment step, since it would significantly simplify the biodiesel production and lower the manufacturing cost.

Mbaraka et al. [22] investigated the use of organic–inorganic hybrid mesoporous silica mono-functionalized with propylsulfonic acid and arenesulfonic acid groups in the esterification reaction of a model feed containing 15 wt% free fatty acid. They observed high esterification activity for both catalysts, but the arenesulfonic acid catalyst was more active, with a conversion above 90% within 60 min. As noted in the work, the reversible esterification reaction appeared to be inhibited by water once the conversion was above 85%. It was concluded that the release of water from the esterification of the free fatty acids limited the extent of the reaction. This effect may have been exacerbated by the hydrophilicity of the reaction environment within the pores of the silica-based catalyst.

An approach to improving the performance of organosulfonic acid-functionalized mesoporous silicas for the esterification of free fatty acid is to create a reaction environment that will continuously exclude water from the mesopores. A method for potentially accomplishing this goal would be the introduction of hydrophobic groups into the mesopores of the organosulfonic acid-functionalized mesoporous silica framework. The hydrophobic organic groups (e.g., allyl and phenyl) would be expected to decrease the amount of water adsorbed into the mesoporous silica [10,23]. These organic groups could be integrated into the mesostructured materials either by grafting onto the preformed mesopores surface or by direct co-condensation during synthesis [23–25].

We describe here the synthesis and characterization of multifunctionalized mesoporous silica materials, which contain both organosulfonic acid and hydrophobic organic groups. These materials were subsequently utilized as catalysts in the esterification reaction of oils with high free fatty acid content as a pretreatment step in the production of biodiesel.

## 2. Experimental

Organosulfonic acid-functionalized mesoporous silicas were synthesized according to a method described previously [5,22,25]. These mesoporous silicas were further modified with hydrophobic organic groups to obtain multifunctionalized mesostructured materials. Tetraethoxysilane (TEOS) (98%, Aldrich) was used as the silica precursor, and (3-mercaptopropyl)trimethoxysilane (MPTMS) (85%, Acros) was used without further purification as the organosulfonic acid source. Pluronic P123 (BASF Co., USA), which is a tri-block copolymer of polyethylene oxide–polypropylene oxide–polyethylene oxide with the molecular structure PEO<sub>20</sub>–PPO<sub>70</sub>–PEO<sub>20</sub>, was used as purchased to tailor the textural properties of the mesoporous materials. The organosulfonic acid-functionalized mesoporous silica was further modified with methyltrimethoxysilane (MeTMS) (95%), ethyltrimethoxysilane (EtTMS) (97%), or phenyltrimethoxysilane (PhTMS) (97%) (purchased from Aldrich) via either a one-step synthesis or a postsynthesis grafting procedure. The organosulfonic acid-functionalized mesoporous material was denoted SBA-15-SO<sub>3</sub>H, and the multifunctionalized mesostructured silica was symbolized by a prefix or suffix to the parent name (SBA-15-SO<sub>3</sub>H), indicating either a postsynthesis grafting or a one-step synthesis procedure, respectively.

### 2.1. One-step synthesis procedure

In a typical one-step synthesis, 4 g of Pluronic P123 was dissolved in 125 ml of 1.9 M HCl at room temperature with stirring and subsequent heating to 40 °C before the addition of TEOS. The TEOS was prehydrolyzed for approximately 45 min before the addition of MPTMS, H<sub>2</sub>O<sub>2</sub>, and a hydrophobic organic precursor. The resulting mixture (molar composition 0.0369 TEOS, 0.0041 MPTMS, 0.0369 H<sub>2</sub>O<sub>2</sub>, and 0.0041 hydrophobic organic group) was agitated for 24 h at 40 °C and thereafter aged for 24 h at 100 °C under static conditions. The resulting solid material was filtered and air-dried. We extracted the template by suspending the solid product in EtOH and refluxing for 24 h. To ensure complete removal of the surfactant, fresh EtOH was introduced after 12 h. The final product was air-dried and then stored in a desiccator.

### 2.2. Post-synthesis grafting procedure

SBA-15-SO<sub>3</sub>H was synthesized as described for the one-step co-condensation procedure with the exclusion of the hydrophobic organic group precursor. The product was collected and subjected to the same template extraction method as discussed above. Prior to incorporation of the hydrophobic organic groups, the solid samples were evacuated overnight at 125 °C. The dried solid (~3 g) was suspended in a mixture of the hydrophobic organosilane (0.004 moles) in 300 ml toluene and refluxed for 4 h. The product was

collected and air-dried overnight, then washed in a Soxhlet extractor with  $\text{CH}_2\text{Cl}_2/\text{Et}_2\text{O}$  for 24 h. The final product was air-dried and then stored in a desiccator.

### 2.3. Characterization

The textural properties of the multifunctionalized mesoporous silica were measured from nitrogen adsorption–desorption isotherms at  $-196^\circ\text{C}$  with a Micromeritics ASAP 2000 system. The surface area and pore size distribution were calculated with the BET and BJH methods, respectively. Prior to measurement, all samples were degassed at  $100^\circ\text{C}$  for 6 h. Powder X-ray diffraction (XRD) analysis of the synthesized samples was performed on a Scintag XDS 2000 diffractometer with a  $\text{Cu-K}\alpha$  radiation source. Organic material present in the solids was determined by elemental analysis performed on a Perkin–Elmer Series II 2400 CHNS analyzer. The organic composition of the modified mesoporous materials was determined by thermogravimetric analysis (TGA) and differential thermoanalysis (DTA) with a Perkin–Elmer TGA7 instrument, with heating from 50 to  $600^\circ\text{C}$  at a rate of  $10^\circ\text{C}/\text{min}$  under air flow. The ion-exchange capacities of the multifunctionalized mesoporous silica were determined by acid–base titration.

The multifunctionalized mesoporous silica were tested for catalytic activity under conditions similar to those described previously [22]. The reagents used for the esterification reaction included palmitic acid ( $\geq 95\%$ , Sigma), refined soybean oil (SBO, Wesson), and methanol ( $\text{MeOH}$ ) ( $\geq 99.9\%$ , Fisher Scientific). The esterification reactions were performed under nitrogen in a high-pressure stainless-steel batch reactor (Eze-Seal, Autoclave Engineers Co., USA) fitted with a mechanical stirrer and a sample outlet. The reaction mixture used in the study had a palmitic acid/SBO weight ratio of 15:85 and a palmitic acid/ $\text{MeOH}$  weight ratio of 1:20. The catalyst loading was equivalent to 10 wt% of the palmitic acid, and the range of reaction temperature studied was from 85 to  $120^\circ\text{C}$ . The reaction mixture was continuously stirred at a rate of 350 rpm.

### 3. Results and discussion

The textural properties of the multifunctionalized organic–inorganic hybrid mesoporous silicas synthesized for the current work are summarized in Table 1. The large BET surface areas of the synthesized multifunctionalized mesoporous silicas were consistent with previous reports [24–26], validating the efficacy of the approach used to extract the surfactant template. The  $\text{N}_2$  adsorption–desorption isotherms of the synthesized samples had Type IV hysteresis loops with sharp adsorption and desorption curves, as seen in Fig. 1, which are consistent with mesoporous materials tailored by nonionic templates [26,27]. The monofunctionalized mesoporous silica (SBA-15- $\text{SO}_3\text{H}$ ), which was the reference catalyst, was synthesized without incorporation

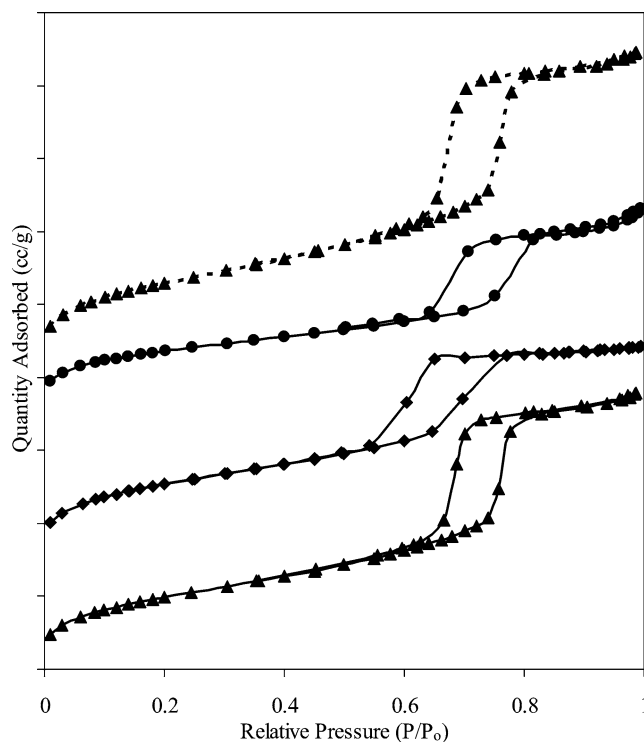


Fig. 1.  $\text{N}_2$  adsorption–desorption isotherms of the multifunctionalized mesoporous materials synthesized by the post-synthesis grafting and co-condensation procedures (( $\blacktriangle$ ) SBA-15- $\text{SO}_3\text{H}$ ; ( $\blacklozenge$ ) SBA-15- $\text{SO}_3\text{H-Et}$ ; ( $\bullet$ ) Et/SBA-15- $\text{SO}_3\text{H}$ ; ( $\blacktriangledown$ ) SBA-15- $\text{SO}_3\text{H}$  after TGA analysis).

of a hydrophobic organic group. The postsynthesis grafting of the hydrophobic organic groups (denoted by the prefix) was performed on a SBA-15- $\text{SO}_3\text{H}$  synthesis batch that was subsequently divided into four samples. Addition of the hydrophobic group to the reference organic–inorganic hybrid mesoporous silica by the grafting technique had no significant effect on the resulting surface area, but the size of the hysteresis loop and pore volume decreased, which implied a possible accumulation of the grafted organic species around the pore openings. The same trend was not observed for samples synthesized by the one-step co-condensation technique. The differences in surface area and pore volume between the reference catalyst and co-condensed multifunctionalized catalysts were insignificant, with the exception of the material multifunctionalized with organosulfonic acid and phenyl (SBA-15- $\text{SO}_3\text{H-Ph}$ ), which underwent a statistically significant decrease in pore volume compared with the other co-condensed samples. Moreover, the  $\text{N}_2$  adsorption–desorption isotherm of SBA-15- $\text{SO}_3\text{H-Ph}$  (not shown) resembled a Type I with a narrow hysteresis loop, suggesting that the pores were not the long cylindrical shape reported for mesoporous materials tailored by nonionic surfactants [23,28]. These features could indicate that the phenyl groups affected the final structure of the mesoporous silica.

The median pore diameters (MPD) of the multifunctionalized organic–inorganic mesoporous silicas synthesized by the postsynthesis grafting procedure and one-step condensation technique were calculated with the BJH method

Table 1  
Textural properties of the multifunctionalized mesoporous silica

Catalysts	Textural properties			C/S (mol/mol)	S (mmol/g)	H <sup>+</sup> (meq/g)
	S <sub>BET</sub> (m <sup>2</sup> /g)	MPD (Å)	V <sub>P</sub> (cm <sup>3</sup> /g)			
SBA-15-SO <sub>3</sub> H (2)	740 ± 40	52 ± 3	0.95 ± 0	5.80	1.00	1.17 ± 0.07
Me/SBA-15-SO <sub>3</sub> H	600	54	0.81	6.58	0.82	1.43
Et/SBA-15-SO <sub>3</sub> H	630	53	0.82	7.98	0.95	1.20
Ph/SBA-15-SO <sub>3</sub> H (2)	520 ± 60	58 ± 1	0.76 ± 0.07	14.07	0.94	0.92 ± 0.04
SBA-15-SO <sub>3</sub> H-Me	810	45	0.91	6.35	0.92	1.30
SBA-15-SO <sub>3</sub> H-Et (4)	770 ± 20	47 ± 4	0.90 ± 0.07	7.97	0.96	1.18 ± 0.10
SBA-15-SO <sub>3</sub> H-Ph	630	34	0.54	12.69	0.98	1.18

on the adsorption branch of the N<sub>2</sub> adsorption–desorption isotherm; these are summarized in Table 1. The pore size distribution of the synthesized samples (not shown) was unimodal for both synthesis techniques. The grafting of the hydrophobic organic groups onto the mesostructure of the reference sample had no significant effect on the pore size distribution; however, the pore volume of the functionalized material decreased. The pore diameter distribution of the Ph/SBA-15-SO<sub>3</sub>H was shifted slightly toward smaller pore diameter when compared with other grafted samples. This difference may indicate that the presence of phenyl groups may have partially blocked the pore openings. In contrast, the hydrophobic organic group incorporated into the mesoporous silica during the one-step co-condensation method seemed to change the pore size distribution relative to the reference catalyst. Therefore, incorporation of the hydrophobic organic groups during the synthesis of the mesoporous silica framework did appear to affect the structure formation of the final mesoporous material.

Replicate syntheses were performed on several of the materials to validate the reproducibility of the textural properties. The catalysts made in replicate are listed in the table, with the number of replicates in parentheses. The standard deviations for their textural properties are tabulated in the table; these were found to be less than 10%.

The influence of hydrophobic organic groups on the mesostructural properties of the organosulfonic acid-functionalized mesoporous silica was studied with XRD. All of the samples showed an intense single peak in the range of 1.6 to 2 degrees, with the exception of the SBA-15-SO<sub>3</sub>H-Ph catalyst, which showed a high degree of disorder. The XRD pattern for materials grafted with hydrophobic groups showed that the anchoring of organosilanes on the mesostructure framework had insignificant consequences for the structure of the final mesoporous catalyst. The same trend was observed for materials synthesized by the co-condensation technique; however, the material was increasingly disordered as the molecular size of the organosilane group increased.

The relative carbon/sulfur ratio and the sulfur content, as determined by elemental analysis, are summarized in Table 1. The equivalence of the sulfur composition in the different samples suggested that the incorporation of hydrophobic groups by either the grafting method or the co-condensation

technique had an insignificant effect on the resulting sulfur content. The mass balance performed on sulfur from the synthesis solution to dry solid (0.95 S mmol/g) was consistent with the elemental analysis, demonstrating a high incorporation yield of the organosulfonic acid precursor. The C/S molar ratio in the reference sample was higher than that expected for only propylsulfonic acid groups. This likely implies that unhydrolyzed methoxy and/or ethoxy groups from the parent MPTMS and TEOS were still present in the synthesized catalyst or that unreacted silanols reacted with ethanol during solvent extraction [24,29]. The C/S ratio was a function of the hydrophobic group incorporated into the mesoporous silica, and the ratio increased as the carbon number of the hydrophobic group increased. The proportionality of the C/S ratio to the carbon number suggested that organosilane addition to the mesoporous silica was not dependent on either the incorporation method or the type of hydrophobic group.

The thermal decomposition of organofunctional groups in the reference sample and mesoporous catalyst functionalized with ethyl and organosulfonic acid (SBA-15-SO<sub>3</sub>H-Et), which was synthesized by the co-condensation method, is shown in Fig. 2. The TGA and DTA analysis of SBA-15-SO<sub>3</sub>H-Et shows weight losses peaks centered at 80 °C, 280 °C, and 460 °C. The first weight loss was assigned to the desorption of water, and the last weight loss, which was also observed in the reference sample, was due to organosulfonic acid decomposition as reported in the literature [24,25,30]. The weight loss at 280 °C was observed only in the multifunctionalized samples. TGA analysis of an as-synthesized SBA-15 sample without the incorporation of any functional groups gave two weight losses at 80 and 190 °C, which were due to water desorption and surfactant decomposition [26]. Propylthiol decomposition has been shown to occur at 350 °C [29,30]. No weight loss was observed at 350 °C for any of the functionalized materials, suggesting that the thiol precursor was converted.

The textural properties of the reference sample (SBA-15-SO<sub>3</sub>H) before and after the TGA analysis were determined with the use of N<sub>2</sub> adsorption–desorption. Following the TGA analysis, the organic functional group was no longer present in the mesoporous material. As shown in Fig. 1, no significant change was observed before and after the thermal removal of organic functional group. Therefore, the presence



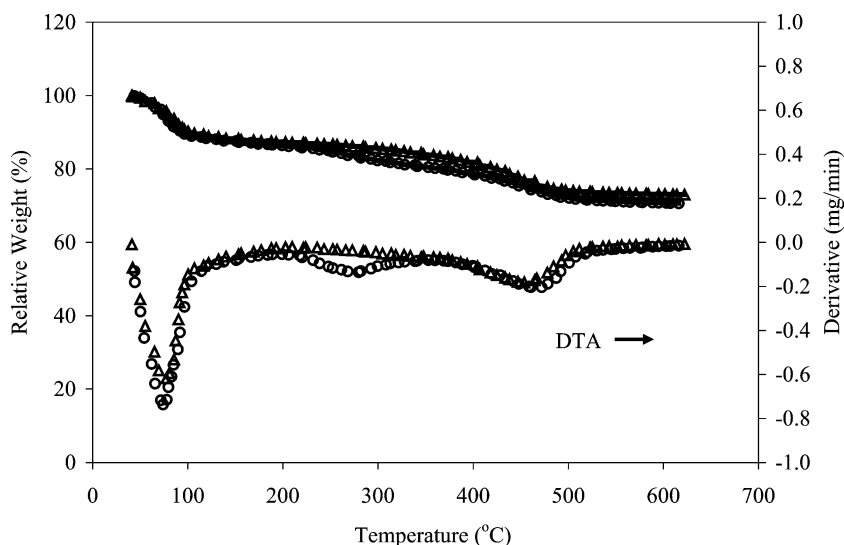


Fig. 2. TGA and DTA analysis of the functionalized mesoporous silica (( $\Delta$ ) SBA-15-SO<sub>3</sub>H; ( $\circ$ ) SBA-15-SO<sub>3</sub>H-Et).

of the organic group in the reference material did not alter the N<sub>2</sub> adsorption–desorption results.

The number of sulfonic acid groups in the catalysts as determined by acid–base titration is given in Table 1. The concentration of sulfonic acid groups for the materials synthesized by the one-step co-condensation technique and the postsynthesis grafting method were in the range of 0.92–1.43 H<sup>+</sup> meq/g sample. The number of acidic sites in the multifunctionalized mesoporous silicas was consistent with that in the reference catalyst and was similar to the number reported previously [22,30]. Therefore, the incorporation of the hydrophobic groups had no significant effect on the concentration of acidic sites in the multifunctionalized samples. The acid–base titration yielded concentrations of sulfonic acid that were about 20% higher than that determined by elemental analysis. This discrepancy could be due to the high ionic strength of the salt solution used in the titration, which would affect the solution pH.

The reaction performance of the catalysts was evaluated by the esterification of a fatty acid in a fatty acid/triglyceride mixture. The results represent an extension of our previous study on the application of organosulfonic acid-functionalized mesoporous silica in the esterification of fatty acids [22]. In that study, we postulated that the production of by-product water in the esterification of palmitic acid with methanol inhibited the esterification reaction. To validate this postulation, the esterification performance of the SBA-15-SO<sub>3</sub>H catalyst was compared for a reaction mixture doped with 3800 ppm (by weight) water and one free of water. Under the reaction conditions used in the present study, the transesterification of triglycerides would be minuscule for an acidic heterogeneous catalyst [14,31]. Shown in Fig. 3 is the palmitic acid weight concentration as a function of reaction time for the water-free and water-doped reactions. The detrimental effect of water on the performance of the organosulfonic acid catalyst was conspicuous, as shown by the decreased palmitic conversion in the water-

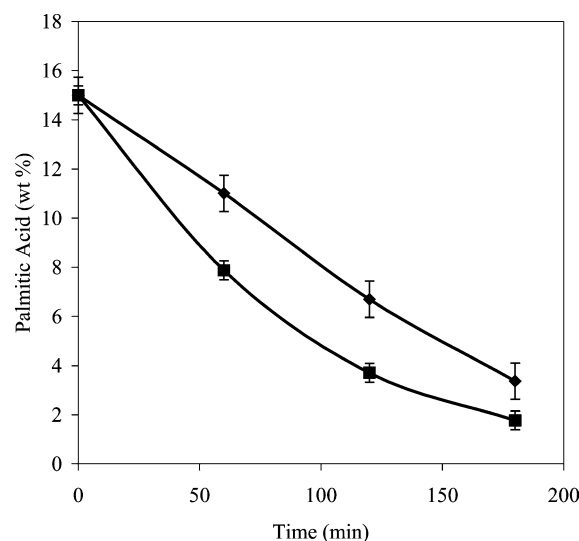


Fig. 3. Effect of water on the esterification reaction of palmitic acid in soybean oil with methanol (85 °C; PA:MeOH = 1:20; Catalyst: 10 wt% SBA-15-SO<sub>3</sub>H; ( $\blacklozenge$ ) 3800 ppm water; ( $\blacksquare$ ) 0 ppm water).

doped reaction system. The negative effect of water has also been reported for esterification reaction catalyzed by homogeneous acidic catalysts, where as little as 0.1 wt% water concentration inhibited the reaction [14,32]. Aafaqi et al. [33] calculated the equilibrium constant for the esterification of palmitic acid with isopropanol from both experimental and thermodynamic data and found that it was 2–10 for a temperature range of 100–170 °C, which demonstrated the reversibility of fatty acid esterification with alcohol. To favor the forward reaction, the esterification of palmitic acid was performed in excess methanol in the current work. The equilibrium effect would be exacerbated by the mesoporous silica catalysts because of the hydrophilicity of the pore interiors, which would lead to an enriched water concentration within the pore. The intention in designing the multifunc-

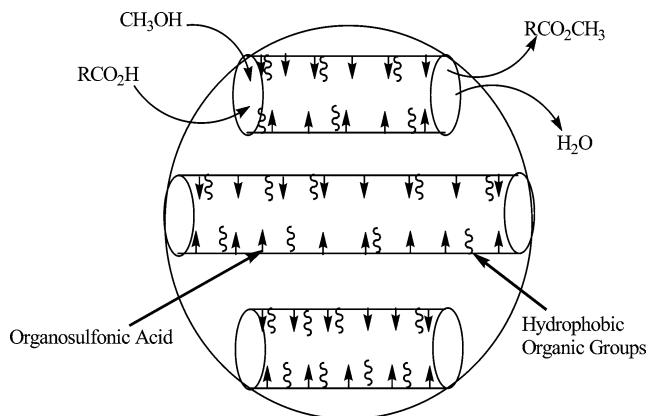


Fig. 4. Schematic of desired water exclusion process with a multifunctionalized mesoporous silica in the esterification of fatty acid with methanol.

tionalized mesoporous silica was to modify the reaction environment adjacent to the propylsulfonic acid catalytic sites inside the mesopores such that the water would be excluded. A proposed schematic of the desired system is shown in Fig. 4. Incorporation of the hydrophobic organic groups into the organosulfonic acid-functionalized mesoporous silica would selectively create an unsuitable environment for water, leading to its exclusion from the active site. Accordingly, the objective of functionalizing the organosulfonic acid mesoporous silica with the inert hydrophobic organic groups was to study the effectiveness of the catalyst in eliminating water from the proximity of the active sites during the esterification of palmitic acid.

To investigate the effect of the incorporation approach on the performance of the catalysts, the hydrophobic organic groups were introduced through either postsynthesis grafting or co-condensation. The results from the esterification reactions catalyzed by the mesoporous silica modified by the two incorporation techniques are shown in Fig. 5. The unmodified SBA-15-SO<sub>3</sub>H gave higher catalytic activity than any of the grafted catalysts with palmitic acid conversions of 88% after 3 h of reaction. In contrast, Et/SBA-15-SO<sub>3</sub>H and Ph/SBA-15-SO<sub>3</sub>H gave the lowest activity, with only 70% conversion after 3 h. These results indicate that the postsynthesis grafting of the hydrophobic groups actually led to a decrease in catalyst performance relative to the reference catalyst. No significant difference between the catalytic performances of the different allyl groups on the multifunctionalized mesoporous silica was observed, despite the differences in their degree of hydrophobicity.

When the same experiments were performed with mesoporous silica multifunctionalized via the co-condensation technique, the results were substantially different, as can be seen in Fig. 5. The co-condensed samples exhibited overall conversion (~84%) after 3 h of reaction similar to that observed with unmodified SBA-15-SO<sub>3</sub>H. However, the co-condensed catalysts gave higher initial catalytic activity, as can be seen after 60 min, where SBA-15-SO<sub>3</sub>H-Ph was the most active and SBA-15-SO<sub>3</sub>H was the least, with 61 and

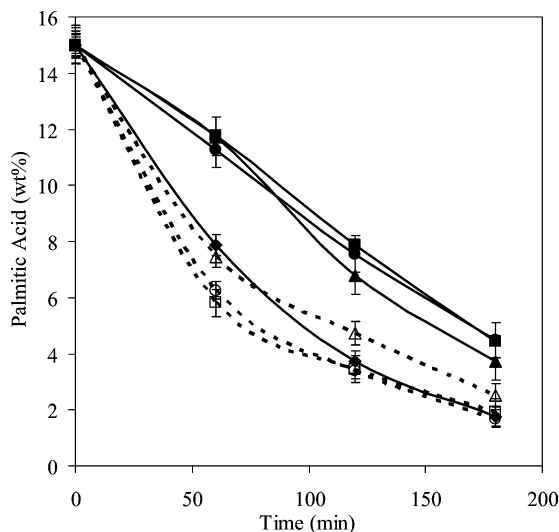


Fig. 5. Catalytic results for the esterification reaction as catalyzed by the grafted and co-condensed multifunctionalized silica (85 °C; PA: MeOH = 1:20; (◆) SBA-15-SO<sub>3</sub>H; (▲) Me/SBA-15-SO<sub>3</sub>H; (●) Et/SBA-15-SO<sub>3</sub>H; (■) Ph/SBA-15-SO<sub>3</sub>H; (△) SBA-15-SO<sub>3</sub>H-Me; (○) SBA-15-SO<sub>3</sub>H-Et; (□) SBA-15-SO<sub>3</sub>H-Ph).

47% palmitic acid conversion, respectively. It is noteworthy that SBA-15-SO<sub>3</sub>H-Ph achieved higher activity despite its apparent inferior textural properties relative to SBA-15-SO<sub>3</sub>H. The reaction results demonstrated that the hydrophobic organic groups did appear to influence the catalytic activity of the hybrid catalysts in the esterification of palmitic acid. Diaz et al. reported similar results for the esterification of glycerol with lauric acid or oleic acid to monoglycerides as catalyzed by multifunctionalized MCM-41 [8].

The results for the grafted and co-condensed catalysts demonstrate that the method of incorporating the inert hydrophobic organosilanes into the mesoporous silica gave dramatically different performance in the esterification of palmitic acid. Shown in Fig. 6 are possible schematics of the catalyst particles resulting from the two incorporation methods. Postsynthesis grafting would likely incorporate the allyl silanes through reaction with surface silanol groups. Because of mass transfer, silanol groups on the outside of the mesoporous particles and at the pore mouth would preferentially react first, creating a hydrophobic exterior on the particle. In contrast, co-condensation would place the organosilanes within the pores, leaving the exterior of the particles hydrophilic. We validated the difference in external particle functionalization for the two incorporation methods by placing the multifunctionalized particles in water. The co-condensed material could be slurried with water, but the postsynthesis grafted particles could not be slurried with water unless methanol was added. This observation suggested that the external surface of the grafted samples was highly hydrophobic, thereby preventing water from accessing the pores.

To further probe the catalytic behavior of the mesoporous silica functionalized via the one-step co-condensation and

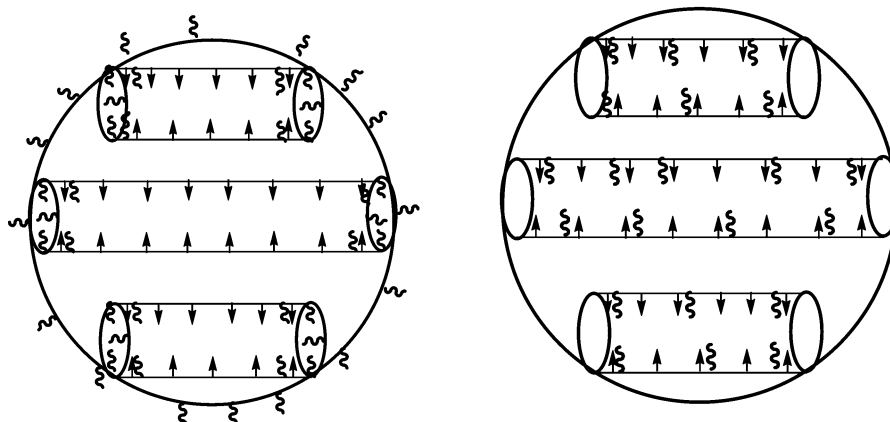


Fig. 6. Schematic comparison of the apparent functionality locations for (a) post-synthesis grafting and (b) one-step co-condensation (~~~~: hydrophobic groups,  $\uparrow$ : propylsulfonic acid sites).

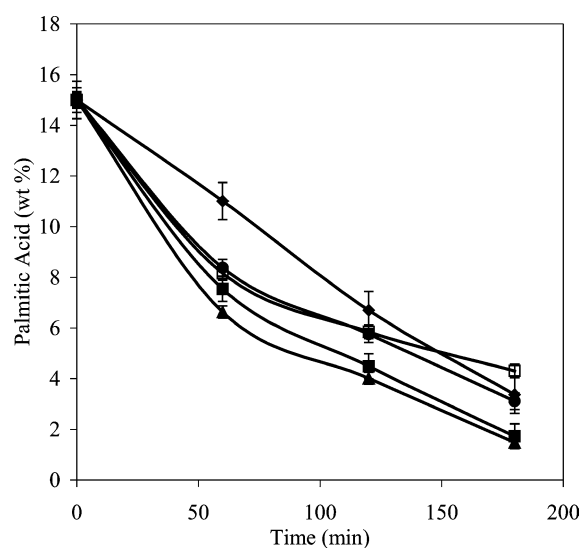


Fig. 7. Catalytic activity of the multifunctionalized silicas resulting from doping 3800 ppm water into the reaction (85 °C; PA:MeOH = 1:20; (◆) SBA-15-SO<sub>3</sub>H; (▲) SBA-15-SO<sub>3</sub>H-Et; (□) SBA-15-SO<sub>3</sub>H-Ph; (●) Et/SBA-15-SO<sub>3</sub>H; (■) Ph/SBA-15-SO<sub>3</sub>H).

the postsynthesis grafting techniques, the esterification reaction was performed in a reaction mixture doped with 3800 ppm water. The reaction results for both monofunctionalized (SBA-15-SO<sub>3</sub>H) and multifunctionalized mesoporous silica catalysts in the presence of added water are shown in Fig. 7. Under these conditions, all of the multifunctionalized mesoporous silicas exhibited higher catalytic activity than the reference catalyst, with conversions of above 80% after 3 h compared with a conversion of only 75% with the reference catalyst. The results demonstrated that the presence of the inert hydrophobic organic groups in the materials allowed the catalysts to sustain higher reaction rates, presumably by selectively preventing water from inhibiting the reaction. Unlike the activity of SBA-15-SO<sub>3</sub>H, which was significantly less in the presence of water doped at 3800 ppm, the activity of the co-condensed catalysts was only slightly lower for the water-doped reaction than for the reaction with

Table 2

Comparison of the kinetic performance of the multifunctionalized mesoporous silica catalysts

Catalyst	Rate constant (min <sup>-1</sup> )			Apparent activation energy (kJ/mol)
	85 °C	100 °C	120 °C	
SBA-15-SO <sub>3</sub> H	$1.0 \times 10^{-2}$	$1.8 \times 10^{-2}$	$2.6 \times 10^{-2}$	$30 \pm 14$
SBA-15-SO <sub>3</sub> H-Et	$1.2 \times 10^{-2}$	$2.1 \times 10^{-2}$	$3.7 \times 10^{-2}$	$40 \pm 2$
SBA-15-SO <sub>3</sub> H-Ph	$6.4 \times 10^{-3}$	$1.1 \times 10^{-2}$	$2.2 \times 10^{-2}$	$40 \pm 1$
Et/SBA-15-SO <sub>3</sub> H	$8.4 \times 10^{-3}$	$1.6 \times 10^{-2}$	$2.4 \times 10^{-2}$	$35 \pm 1$
Ph/SBA-15-SO <sub>3</sub> H	$1.5 \times 10^{-2}$	$1.9 \times 10^{-2}$	$1.9 \times 10^{-2}$	$10 \pm 1$

no water added. This result further supports the assertion that creating a hydrophobic environment within the pores served to exclude water from the active sites. Unexpectedly, the activity of the grafted samples with the water-doped reaction system actually improved relative to the reaction system that was free of water. The improvement in activity with water doping for the grafted system was such that the grafted catalysts were now found to outperform the reference SBA-15-SO<sub>3</sub>H catalyst.

Determining the cause of the performance enhancement of the grafted samples in the presence of excess water requires an understanding of the relative importance of the location of the hydrophobic organic groups and their relationship with the reactants, since both of these attributes could contribute to the improved performance. To better understand these features, reactions with 3800 ppm water-doped mixtures were performed at temperatures from 85 to 120 °C. These data were then used to calculate apparent activation energies for the catalysts, assuming a pseudo-first-order reaction with respect to palmitic acid, as discussed previously [22]. The calculated rate constants and apparent activation energies are summarized in Table 2 for the monofunctionalized and multifunctionalized mesoporous silica catalysts. A temperature increase of 15–20 °C caused approximately a doubling of the rate constants in all of the catalysts except Ph/SBA-15-SO<sub>3</sub>H. The range of activation energies for the monofunctionalized and multifunctionalized

mesoporous silica catalysts was consistent with the range reported for propylsulfonic acid SBA-15 materials tailored with Pluronic P123 [22]. A similar activation energy for the esterification reaction of palmitic acid with alcohol has been reported [33]. The low activation energy of Ph/SBA-15-SO<sub>3</sub>H was possibly due to external mass transfer limitation resulting from a strong interaction between the phenyl group and the reactants around the pore mouth.

Dixit et al. [34] studied the solution behavior of alcohols under strict anhydrous conditions and in the presence of low water levels. They observed with anhydrous methanol that the hydroxyl groups of adjacent methanol molecules interact with each other through hydrogen bonding, leading to oligomeric-type chains, which behave as hydrophobic compounds because of their conformation. These hydrogen bonding-derived chains were completely broken upon the addition of only ppm levels of water. A similar phenomenon may be playing a role in the esterification reaction system. The esterification reaction mixture consists mainly of amphiphilic reactants (palmitic acid and methanol) and soybean oil, which in analogy to the methanol study could form long hydrophobic chains. The bulky chains of palmitic acid could then limit the accessibility of the catalytic active sites because of blockage of the mesopores. To minimize the external mass transfer limitations of the reactants with the catalysts, the hydrophobic chains of the reactants would need to be eliminated. One approach to breaking the chains would be to introduce a strong polar compound into the reaction mixture, which would then interact with the hydroxyl groups of the amphiphilic compounds. The presence of water molecules in the reaction mixture or the existence of silanols on the external surface area of the mesoporous catalysts could disrupt the solution chains. The higher performance of the catalysts synthesized via the one-step co-condensation technique in the esterification reaction of palmitic acid without the addition of excess water may suggest that the external surface area was sufficiently hydrophilic because of the presence of surface hydroxyl groups. As a result, the esterification reaction occurred within the mesopores, where the reactants were catalyzed by the organosulfonic acid and the water produced was excluded from the catalytic site by the hydrophobic organic groups. However, the postsynthesis grafting method had the opposite effect on the mesoporous catalysts, that is, high concentrations of the hydrophobic organic groups could be found on the external surface area while the organosulfonic acid was in the interior of the mesopores. Consequently, in the water-free reaction system the reactant chains were maintained, resulting in poor diffusion of reactants into the mesopores and thus low conversions of palmitic acid. As demonstrated in Fig. 7, the addition of water into the reaction mixture with the grafted catalyst gave reaction rates higher than those observed in the absence of water, which may be attributed to improved accessibility of the reactive sites through disruption of the solution chains.

To determine the effect of water concentration on the esterification of palmitic acid with methanol as catalyzed by

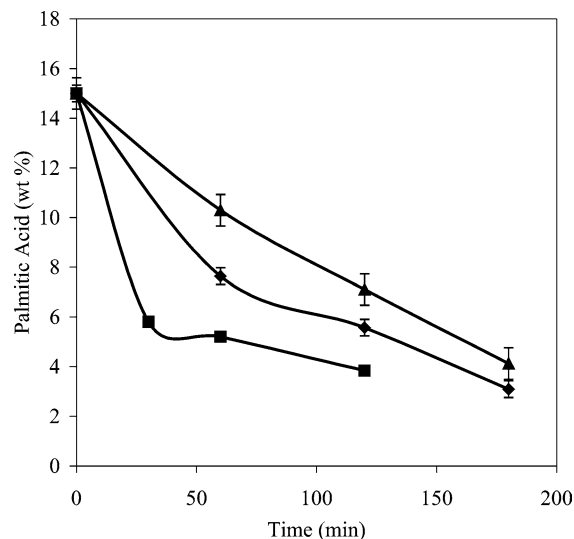


Fig. 8. Effect of water doping on the catalytic activity of Et/SBA-15-SO<sub>3</sub>H (85 °C; PA:MeOH = 1:20; (▲) 0 ppm; (◆) 3800 ppm; (■) 1200 ppm).

Et/SBA-15-SO<sub>3</sub>H, the reaction system was doped with different amounts of water; the reaction results are shown in Fig. 8. As seen in the figure, doping with 1200 ppm water gave the highest conversion of 74% after 2 h, followed by doping with 3800 ppm water, with a conversion of 62% after 2 h. The least active was the system in which no water was introduced prior to reaction, which achieved a conversion of only 52% after 2 h. The results were consistent with water inhibiting the esterification reaction, as demonstrated by the loss in activity when water doping was increased from 1200 to 3800 ppm. However, the presence of a small concentration of water in the reaction mixture enhanced the performance of the catalysts, which was consistent with the speculated chain formation mechanism discussed above. It is interesting to note that the activity of the grafted catalyst diminished significantly by 12% upon the change of water doping from 1200 to 3800 ppm, whereas the performance of the co-condensed catalyst functionalized with an ethyl group decreased only slightly (by less than 1%) when the water doping was increased from 0 to 3800. These results were further indirect confirmation that the co-condensed catalysts led to hydrophobic environments within the pores, whereas the grafted catalysts still had significant hydrophilicity within the pores.

The proposed solution effects due to hydrogen bonding would be expected to be less pronounced at higher temperatures, so a final set of experiments was performed at 120 °C with 25 wt% palmitic acid in soybean oil. The results for these experiments are shown in Fig. 9. All of the multifunctionalized catalysts, with the exception of Ph/SBA-15-SO<sub>3</sub>H, were more active than the monofunctionalized acid catalysts, achieving palmitic acid conversion above 99% after 2 h. The high catalytic activity of the Et/SBA-15-SO<sub>3</sub>H is consistent with the assumption that at high reaction temperature, the hydrophobic chains are eliminated because of the absence of hydrogen bonding. The low catalytic perfor-



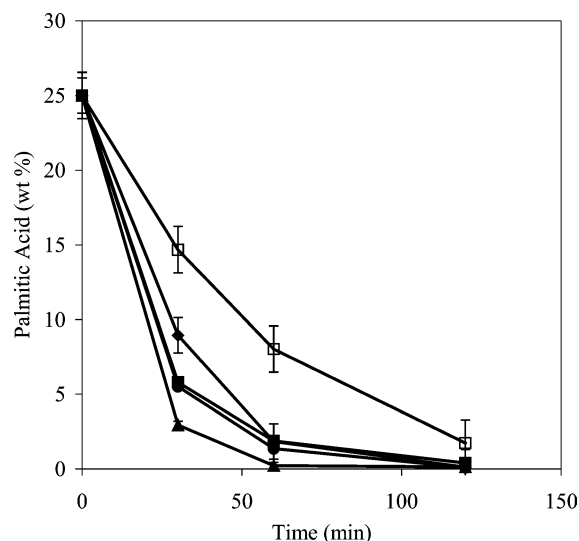


Fig. 9. Catalytic results for the esterification of 25 wt% palmitic acid in soybean oil catalyzed by the multifunctionalized silicas (120 °C; PA: MeOH = 1:20; (◆) SBA-15-SO<sub>3</sub>H; (●) SBA-15-SO<sub>3</sub>H-Et; (■) SBA-15-SO<sub>3</sub>H-Ph; (▲) Et/SBA-15-SO<sub>3</sub>H; (□) Ph/SBA-15-SO<sub>3</sub>H).

mance of the Ph/SBA-15-SO<sub>3</sub>H catalyst in the esterification reaction is consistent with the apparent activation energy results given in Table 2. The higher temperature results confirm that the addition of the hydrophobic organic groups to the structure of the mesoporous silica modifies the catalytic environment so that water produced by the reaction is excluded, permitting higher catalytic conversions.

#### 4. Conclusion

Mesoporous silica multifunctionalized with both organosulfonic acid and hydrophobic organic groups was shown to be effective in esterifying free fatty acid while excluding water, which is an undesired reaction product, from the proximity of the active sites. Both postsynthesis grafting and one-step co-condensation techniques were used to introduce the hydrophobic organic groups, with the techniques preferentially modifying the external and internal surface areas, respectively. It was shown that the technique of incorporating the hydrophobic organic group into the mesoporous silica and knowledge of the reaction mixture are important to the enhancement of the performance of the catalysts. This work demonstrates the potential of utilizing organic–inorganic hybrid mesoporous materials for the rational design of heterogeneous catalysts at the molecular scale.

#### Acknowledgments

This material is based upon work supported by the Cooperative State Research, Education, and Extension Service,

U.S. Department of Agriculture, under Agreement Nos. 2002-34188-12035 and 2004-34188-15067.

#### References

- [1] A. Stein, B.J. Melde, R.C. Schroden, *Adv. Mater.* 12 (2000) 1403.
- [2] J.Y. Ying, C.P. Mehnert, M.S. Wong, *Angew. Chem. Int. Ed.* 38 (1999) 56.
- [3] G.J.A. Soler-Illia, C. Sanchez, B. Lebeau, J. Patarin, *Chem. Rev.* 102 (2002) 4093.
- [4] A.P. Wight, M.E. Davis, *Chem. Rev.* 102 (2002) 3589.
- [5] J.A. Melero, G.D. Stucky, R. van Grieken, G. Morales, *J. Mater. Chem.* 12 (2002) 1664.
- [6] W.D. Bossaert, D.E. De Vos, W.M. Van Rhijin, J. Bullen, P.J. Grobet, P.A. Jacobs, *J. Catal.* 182 (1999) 156.
- [7] W.M. Van Rhijin, D.E. De Vos, W.D. Bossaert, P.A. Jacobs, *Chem. Commun.* (1998) 317.
- [8] I. Diaz, C. Marquez-Alvarez, F. Mohino, J. Perez-Pariente, E. Sastre, *J. Catal.* 193 (2000) 295.
- [9] V. Lin, C.-Y. Lai, J. Huang, S.-A. Song, S. Xu, *J. Am. Chem. Soc.* 123 (2001) 11510.
- [10] M. Park, S. Komarneni, *Micropor. Mesopor. Mater.* 25 (1998) 75.
- [11] R.C. Brown, *Biorenewable Resources*, Iowa State Press Ames, 2003.
- [12] H.N. Basu, M.E. Norris, U.S. Patent 5,525,126 (1996).
- [13] M. Canakci, J. Van Gerpen, *Trans. ASAE* 44 (2001) 1429.
- [14] M. Canakci, J. Van Gerpen, *Trans. ASAE* 42 (1999) 1203.
- [15] F. Ma, M.A. Hanna, *Biores. Technol.* 70 (1999) 1.
- [16] A.K. Agarwal, L.M. Das, *Trans. ASME* 123 (2001) 440.
- [17] M.J. Haas, K.M. Scott, T.L. Alleman, R.L. McCormick, *Energy Fuels* 15 (2001) 1207.
- [18] J.M. Encinar, J.F. Gonzalez, E. Sabio, M.J. Ramiro, *Ind. Eng. Chem. Res.* 38 (1999) 2927.
- [19] S. Gryglewicz, *Biores. Technol.* 70 (1999) 249.
- [20] D.G.B. Boocock, S.K. Konar, V. Mao, C. Lee, S. Buligan, *J. Am. Oil Chem. Soc.* 75 (1998) 1167.
- [21] S. Koono, O. Moriya, T. Noguchi, H. Okamura, EP Patent 566,047 (1993).
- [22] I.K. Mbaraka, D.R. Radu, V.S.-Y. Lin, B.H. Shanks, *J. Catal.* 219 (2003) 329.
- [23] A. Bhaumik, T. Tatsumi, *J. Catal.* 189 (2000) 31.
- [24] I. Diaz, C. Marquez-Alvarez, F. Mohino, J. Perez-Pariente, E. Sastre, *J. Catal.* 193 (2000) 283.
- [25] D.I. Margolese, J.A. Melero, S.C. Christiansen, B.F. Chmelka, G.D. Stucky, *Chem. Mater.* 12 (2000) 2448.
- [26] M. Kruk, M. Jaroniec, C.H. Ko, R. Ryoo, *Chem. Mater.* 12 (2000) 1961.
- [27] W. Zhang, B. Glomski, T.R. Pauly, T.J. Pinnavaia, *Chem. Commun.* (1999) 1803.
- [28] S.H. Joo, R. Ryoo, M. Kruk, M. Jaroniec, *J. Phys. Chem. B* 106 (2002) 4640.
- [29] I. Diaz, C. Marquez-Alvarez, F. Mohino, J. Perez-Pariente, E. Sastre, *Micropor. Mesopor. Mater.* 44–45 (2001) 295.
- [30] I. Diaz, F. Mohino, J. Perez-Pariente, E. Sastre, *Appl. Catal. A* 242 (2003) 161.
- [31] B. Freedman, E.H. Pryde, T.L. Mounts, *J. Am. Oil Chem. Soc.* 61 (1984) 1638.
- [32] D. Kusdiana, S. Saka, *Biores. Technol.* 91 (2004) 289.
- [33] R. Aafaqi, A.R. Mohamed, S. Bhatia, *J. Chem. Tech. Biotech.* 79 (2004) 1127.
- [34] S. Dixit, J. Crain, W.C.K. Poon, J.L. Finney, A.K. Soper, *Nature* 416 (2002) 829.